Atoms **2014**, *2*, 225-252; doi:10.3390/atoms2020225

OPEN ACCESS

atoms

ISSN 2218-2004

www.mdpi.com/journal/atoms

Article

Widths and Shifts of Isolated Lines of Neutral and Ionized Atoms Perturbed by Collisions With Electrons and Ions: An Outline of the Semiclassical Perturbation (SCP) Method and of the Approximations Used for the Calculations

Sylvie Sahal-Bréchot [1,*], Milan S. Dimitrijević [1,2] and Nabil Ben Nessib [3]

[1] Laboratoire d'Étude du Rayonnement et de la Matière en Astrophysique et Atmosphères (LERMA2), Observatoire de Paris, UMR CNRS 8112, UPMC, 5 Place Jules Janssen, 92195 Meudon CEDEX, France

[2] Astronomical Observatory, Volgina 7, 11060 Belgrade, Serbia; E-mail: mdimitrijevic@aob.rs

[3] Department of Physics and Astronomy, College of Science, King Saud University. Riyadh 11451, Saudi Arabia; E-mail: nbennessib@ksu.edu.sa

* Author to whom correspondence should be addressed; E-Mail: sylvie.sahal-brechot@obspm.fr; Tel.: +331-450-774-42; Fax: +331-450-771-00.

Received: 24 April 2014; in revised form: 22 May 2014 / Accepted: 26 May 2014 / Published: 10 June 2014

Abstract: "Stark broadening" theory and calculations have been extensively developed for about 50 years. The theory can now be considered as mature for many applications, especially for accurate spectroscopic diagnostics and modeling, in astrophysics, laboratory plasma physics and technological plasmas, as well. This requires the knowledge of numerous collisional line profiles. In order to meet these needs, the "SCP" (semiclassical perturbation) method and numerical code were created and developed. The SCP code is now extensively used for the needs of spectroscopic diagnostics and modeling, and the results of the published calculations are displayed in the STARK-B database. The aim of the present paper is to introduce the main approximations leading to the impact of semiclassical perturbation method and to give formulae entering the numerical SCP code, in order to understand the validity conditions of the method and of the results; and also to understand some regularities and systematic trends. This would

also allow one to compare the method and its results to those of other methods and codes. [1]

Keywords: Stark broadening; impact approximation; isolated lines; semiclassical perturbation picture

1. Introduction

"Stark broadening" theory and calculations have been extensively developed for about 50 years. Following the pioneering work by [1–4], the theory and calculation of collisional line broadening in the impact approximation showed a great expansion from the sixties. The theory can now be considered as mature for many applications, especially for accurate spectroscopic diagnostics and modeling, in astrophysics, laboratory plasma physics and technological plasmas, as well. This requires the knowledge of numerous collisional line profiles. Hence, calculations based on a simple method that is accurate and fast enough are necessary for obtaining numerous results. In order to meet these needs, the impact semiclassical perturbation (SCP) method and the associated numerical code were created and developed by Sahal-Bréchot for isolated lines in the sixties and seventies [5–9], then updated [10–12] in the eighties and nineties and then, again, in the present new century [13]. Since the impact approximation was assumed, the method was inspired by the developments of the theory of electron-atom and electron-ion collisions which have been rapidly expanding since the sixties. In particular [14], the semiclassical perturbation method appeared to be especially suitable, due to the speed of the numerical calculations and to the sufficient expected accuracy. Nowadays, the SCP code is extensively used for the needs of spectroscopic diagnostics and modeling, and the results of the published calculations are displayed in the STARK-B database [15].

The aim of the present paper is to introduce the main approximations leading to the impact semiclassical perturbation method and to the formulae entering the numerical SCP code. This would give an idea of the validity conditions of the method and of the results, which are discussed in Section 4. This would also allow one to compare the different codes, and this would help to understand some regularities and systematic trends observed in the experiments and in the results of calculations.

In the next section, we will recall the basic key assumptions leading to the theory of collisional line broadening in impact approximation. We will define the concepts of "complete collision" approximation and of "isolated lines". Then, we will recall the specific approximations made in the semiclassical perturbation treatment for isolated lines of neutral and ionized atoms perturbed by electrons and positive ions in the impact approximation. We will give the formulae entering the SCP numerical code. Then, we will discuss the approximations made and the obtained results. This would allow one to compare

[1] The content of the present paper was presented and discussed at the first Spectral Line Shapes in Plasmas (SLSP) code comparison Workshop, which was held in Vienna, Austria, April 2–5, 2012.

the results obtained by other numerical codes and to understand some regularities and systematic trends observed in the experiments and in the results of calculations.

2. Collisional Line Broadening in the Impact Approximation

Following the pioneering work by Baranger [1–4], the theory and calculation of collisional line broadening widths and shifts in the impact approximation for electrons and ion interactions is very briefly outlined in the following.

We consider a neutral or ionized atom surrounded by the perturbers, P, moving around it. We begin with the very general formula [1–4], which gives the intensity, $I(\omega)$, of a spectral line ($i \rightarrow f$) at the angular frequency, ω:

$$I(\omega) = \frac{4\omega^4}{3c^3} |\langle f \,|\mathbf{d}|\, i\rangle|^2 \tag{1}$$

$$I(\omega) = \frac{1}{2\pi} \int_{-\infty}^{+\infty} \exp\left(\mathrm{i}\omega s\right)\, \Phi(s)\mathrm{ds}. \tag{2}$$

Dropping the factor, $4\omega^4/3c^3$, the autocorrelation function $\Phi(s)$ reads:

$$\Phi(s) = \mathrm{Tr}\left[\mathbf{d}\, T^*(s)\, \mathbf{d}\, T(s)\, \rho\right]. \tag{3}$$

Here, ρ is the density matrix of the whole system atom (A) surrounded by the bath of particles (B: photons R and perturbers P), **d** is the dipole moment, $I(\omega)$ is the Fourier transform of the autocorrelation function, $\Phi(s)$, and $T(s)$ is the evolution operator of the whole system. Tr is the trace over the states of the whole system and c is the velocity of the light.

• With the *no-back reaction approximation*, which is the first key approximation, the bath, B, remains described by its unperturbed density operator (or its distribution function in the classical picture), irrespective of the amount of energy and polarization diffusing into it from A:

$$\rho(t) = \rho_A(t) \otimes \rho_B(t).$$

It is also assumed that the bath, B, is in a stationary state, and thus, $\rho_B(t) = \rho_B$. We also suppose that the bath of colliding perturbers P (density matrix ρ_P) is decoupled from the bath of photons R (density matrix ρ_R). Thus:

$$\rho_B = \rho_P \otimes \rho_R,$$

and we will only consider in the following the interaction with the bath of colliding particles. Hence, we can write:

$$\Phi(s) = \mathrm{Tr}_A\left[\rho_A\, \mathrm{Tr}_P[\mathbf{d}\, T^*(s)\, \mathbf{d}\, T(s)\, \rho_P\,]\right] \tag{4}$$

where Tr_A is the trace over the atomic states and Tr_P is a trace over all the perturbers. When the perturbers can be treated classically, the trace over the perturbers is replaced by a statistical average $[...]_{AV}$ over all modes of motion of the perturbers, which move on a classical path [4]:

$$\Phi(s) = \mathrm{Tr}_A\left[\rho_A\, \mathbf{d}\, T^*(s)\, \mathbf{d}\, T(s)\right]_{AV}. \tag{5}$$

• The second key approximation is the *impact approximation*: the interactions are separated in time. In other words, the atom interacts with one perturber only at a given time: the mean duration, τ, of an interaction must be much smaller than the mean interval between two collisions, ΔT. This can be expressed as:

$$\tau \ll \Delta T,$$

where $\tau \approx \frac{\rho_{typ}}{v_{typ}}$, ρ_{typ} is a mean typical impact parameter and v_{typ} a mean typical relative velocity.

ΔT is of the order of the inverse of the collisional line width, which can be very roughly written as equal to $N_P v_{typ} \rho_{typ}^2$, where N_P is the density of the perturbers.

Thus, the validity condition of the impact approximation can be written as:

$$\rho_{typ} << N_P^{-1/3}. \tag{6}$$

The "collision volume", of the order of ρ_{typ}^3, must be smaller than N_P^{-1}, the volume per perturber [1]. In other words, the perturbers are independent and their effects are additive.

• Then, we will make the *complete collision approximation*: within this approximation, atom–radiation and atom–perturber interactions are decoupled. This implies that the collision must be considered as instantaneous in comparison with the time, Γ^{-1}, characteristic of the evolution of the excited state under the effect of the interaction with the radiation. In other words, the interaction process has time to be completed before the emission of a photon.

The complete collision approximation can become invalid in line wings, even if it remains valid in the line center. Its condition of validity is:

$$\tau << 1/\Delta\omega,$$

where $\Delta\omega$ is the detuning.

Then, using Equation (4) in the quantum picture or Equation (5) in the semiclassical picture, the calculation of the line profile becomes an application of the theory of atomic collisions. This implies that we have to express and calculate the scattering S-matrix.

• In addition, in the case of *isolated lines* (*cf.* Figure 1), which implies that neighboring levels do not overlap [3], the line profile, $F(\omega)$, between the levels, i, $(\alpha_i J_i)$ and f $(\alpha_f J_f)$, is Lorentzian:

$$I(\omega) = \rho_A (\alpha_i J_i) \frac{4\omega^4}{3c^3} F(\omega) \tag{7}$$

$$F(\omega) = \frac{1}{\pi} \int_0^\infty \mathrm{e}^{i(\omega-\omega_{if})s} \Phi(s) \, \mathrm{d}s \tag{8}$$

$$\Phi(s) = \exp(-(w + \mathrm{i}d) s) \tag{9}$$

and

$$F(\omega) = \frac{w}{\pi \left[(\omega - \omega_{if} - d)^2 + w^2\right]} \tag{10}$$

ρ_A is the reduced atomic density matrix at the stationary state.

Figure 1. The studied line, $i - f$ (red-bold arrow, example of an emission line): $\alpha_i J_i$ is the initial level, and $\alpha_f J_f$ is the final level. The perturbing levels are αJ, $\alpha' J'$. Black-thin arrows: the inelastic transitions in excitation and deexcitation. The levels are broadened (grey strips), but do not overlap.

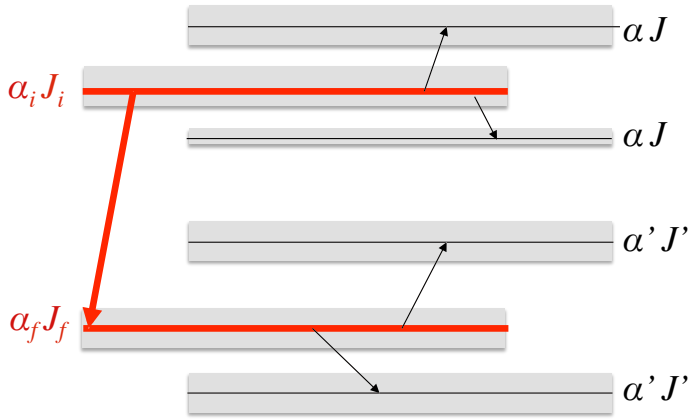

• The determination of the atomic density matrix elements (the populations of the levels) deserves special attention. In fact, Baranger [1–4] assumes LTE (local Thermodynamical equilibrium), and then, $\rho_A(\alpha_i J_i)$ is the Boltzmann factor:

$$\rho_A(\alpha_i J_i) = g_i \frac{\exp\left(-\frac{E_i}{kT}\right)}{Z(T)} \tag{11}$$

where g_i is the statistical weight of the $(\alpha_i J_i)$ level, E_i its energy, k the Boltzmann constant and $Z(T)$ the partition function at the temperature, T.

Out of LTE, it is more complicated, because the calculation of the profile and of the populations are not decoupled for obtaining the intensity of the line. In particular, (7) is no longer valid. This is the problem of the *redistribution of radiation*, which has been extensively studied for many years, especially for the study of stellar atmospheres [16–18] and some laboratory plasmas.

However, within the complete redistribution approximation, the calculation of the line profile and of the populations become decoupled, and (7) is again valid. This needs to assume that the radiation is weak (the atom-radiation interaction is treated with the second-order perturbation theory) and to make the *Markov approximation*: the time evolution of $\rho_A(t)$ does not depend on its past history and only depends on the time, t.

The coupling of the atomic density matrix and the line profile needs to go beyond the Markov approximation, but this is outside the scope of the present theory. See, for instance, [18].

Consequently, out of LTE, within the complete redistribution approximation, the statistical equilibrium equations for a collisional radiative model can be solved for obtaining the populations by ignoring the line profiles, and then, the resulting populations are multiplied to the line profile given by Equation (8) for obtaining the intensity.

We now concentrate our attention on the determination of the line profile given by (10). We will determine the half-width, w (half width at half-maximum intensity), and the shift, d, of the profile of the $i - f$ line. They are given by:

$$w + \mathrm{i}d = \mathrm{Tr}_P \left(1 - S_{ii}\, S^*_{ff}\right) \tag{12}$$

where the trace over the perturbers, Tr_P, is given by:

$$Tr_P = N_P \int_0^\infty v\, f(v) dv \int_0^\infty 2\pi\, \rho\, \mathrm{d}\rho \oint \frac{\mathrm{d}\Omega}{4\pi}. \tag{13}$$

Equation (13) is written in the semiclassical picture, where the colliding perturbers move along a classical path of impact parameter ρ, but this is not essential. Here, v is the relative velocity of the perturber, $f(v)$ the distribution of velocities (Maxwell distribution) and N_P the density of the perturbers.

$$\oint \frac{\mathrm{d}\Omega}{4\pi}$$

is the angular average over all directions of the colliding perturbers. Hence:

$$w + \mathrm{i}d = N_P \int_0^\infty v\, f(v) dv \int_0^\infty 2\pi\, \rho\, \mathrm{d}\rho \left\langle 1 - S_{ii}\, S^*_{ff} \right\rangle_{angular\ average} \tag{14}$$

This angular average is a linear combination of products of "3-j" coefficients and of initial and final Zeeman states of the S-matrix elements [3]. Thus, Equation (14) reads:

$$\begin{aligned} w + \mathrm{i}d &= N_P \int_0^\infty v\, f(v) dv \int_0^\infty 2\pi\, \rho\, \mathrm{d}\rho \\ &\times \Big[1 - \sum_{\substack{M_i\, M'_i \\ M_f\, M'_f \\ \mu}} (-1)^{2J_f + M_f + M'_f} \begin{pmatrix} J_i & 1 & J_f \\ -M_i & \mu & M_f \end{pmatrix} \begin{pmatrix} J_i & 1 & J_f \\ -M'_i & \mu & M'_f \end{pmatrix} \\ &\times \left\langle \alpha_f J_f M_f \left| S^* \right| \alpha_f J_f M'_f \right\rangle \left\langle \alpha_i J_i M_i \left| S \right| \alpha_i J_i M'_i \right\rangle \Big] \end{aligned} \tag{15}$$

This is the basic "Baranger's formula" which gives the half-width and the shift of an isolated line perturbed by collisions (*i.e.*, impact and complete collision approximation). We notice that the S-matrix is symmetric, unitary and can be calculated in any reference frame. Its matrix elements have to be calculated for a given relative velocity, v, and an impact parameter, ρ, in the semiclassical description. This will appear in the following equations.

In fact, the T-matrix, where $T = 1 - S$ (and, thus, $T^*T = 2Re(T)$), is used in the SCP method. Thus, we will use it in the following.

After elementary calculations using the properties of the "3-j" coefficients, Equation (15) reads:

$$\begin{aligned} w + \mathrm{i}d &= N_P \int_0^\infty v\, f(v) dv \int_0^\infty 2\pi\, \rho\, \mathrm{d}\rho \\ &\times \Bigg[\sum_{M_i} \frac{1}{2J_i+1} \left\langle \alpha_i J_i M_i \right| T(\rho, v) \left| \alpha_i J_i M_i \right\rangle + \sum_{M_f} \frac{1}{2J_f+1} \left\langle \alpha_f J_f M_f \right| T^*(\rho, v) \left| \alpha_f J_f M_f \right\rangle \\ &\quad - \sum_{\substack{M_i\, M'_i \\ M_f\, M'_f \\ \mu}} (-1)^{2J_f + M_f + M'_f} \begin{pmatrix} J_i & 1 & J_f \\ -M_i & \mu & M_f \end{pmatrix} \begin{pmatrix} J_i & 1 & J_f \\ -M'_i & \mu & M'_f \end{pmatrix} \\ &\quad \times \left\langle \alpha_i J_i M_i \right| T(\rho, v) \left| \alpha_i J_i M'_i \right\rangle \left\langle \alpha_f J_f M_f \right| T^*(\rho, v) \left| \alpha_f J_f M'_f \right\rangle \Bigg] \end{aligned} \tag{16}$$

Then, the half-width at half-maximum intensity w, and the full width at half-maximum intensity $W = 2w$ become:

$$\begin{aligned} W = 2w = N_P \int v\, f(v) \mathrm{d}v \\ \times \left[\left(\sum_{\alpha J} \sigma\left(\alpha_i J_i \to \alpha J, v\right) + \sum_{\alpha' J'} \sigma\left(\alpha_f J_f \to \alpha' J', v\right) \right) \right. \\ - 2\mathrm{Re} \int_0^\infty 2\pi\, \rho\, \mathrm{d}\rho \left[\sum_{\substack{M_i\, M_i' \\ M_f\, M_f' \\ \mu}} (-1)^{2J_f + M_f + M_f'} \right. \\ \times \begin{pmatrix} J_i & 1 & J_f \\ -M_i & \mu & M_f \end{pmatrix} \begin{pmatrix} J_i & 1 & J_f \\ -M_i' & \mu & M_f' \end{pmatrix} \\ \left. \left. \times \left\langle \alpha_f J_f M_f \left| T^*(\rho, v) \right| \alpha_f J_f M_f' \right\rangle \left\langle \alpha_i J_i M_i \left| T(\rho, v) \right| \alpha_i J_i M_i' \right\rangle \right] \right. \end{aligned} \tag{17}$$

In Equation (17):

$$\sum_{\alpha J} \sigma\left(\alpha_i J_i \to \alpha J, v\right)$$

is a sum of all the inelastic cross-sections originating from the initial level towards all perturbing levels, αJ, in excitation and deexcitation (*cf.* Figure 1), with $\alpha_i J_i \neq \alpha J$, and of the elastic cross-section $\sigma(\alpha_i J_i \to \alpha_i J_i, v)$.

In fact:

$$\sigma\left(\alpha_i J_i \to \alpha J, v\right) = \int_0^\infty 2\pi\, \rho\, \mathrm{d}\rho\, P(\alpha_i J_i \to \alpha J,\ \rho,\ v) \tag{18}$$

where $P(\alpha_i J_i \to \alpha J,\ \rho,\ v)$ is the transition probability between the levels, $(\alpha_i J_i)$ and (αJ), for the impact parameter, ρ, and the relative velocity, v.

We have similar expressions for the inelastic cross-sections originating from the final level $\alpha_f J_f$. Then the perturbing levels are $\alpha' J'$ and the elastic cross-section is $\sigma(\alpha_f J_f \to \alpha_f J_f, v)$.

We notice that the transition probability:

$$P(\alpha_i J_i \to \alpha J,\ \rho,\ v) = \frac{1}{2J_i + 1} \sum_{M_i\, M} \left| \left\langle \alpha_i J_i M_i \left| T(\rho, v) \right| \alpha J M \right\rangle \right|^2 \tag{19}$$

is a sum over the final M substates and an average over the initial M_i substates of the T-matrix elements.

The third term of Equations (16) and (17) is the so-called "interference term", which is a linear combination of off-diagonal elastic elements of the initial and final elastic elements of the T-matrix. For collisions with electrons, it is often small (10% of the total width or thereabout), but not always.

Equations (16) and (17) will be used in the SCP method and numerical code.

Finally, we notice that the fine structure (and, *a fortiori*, hyperfine structure) can generally be ignored, and consequently, the fine structure components (or hyperfine components) have the same width and the same shift, which are equal to those of the multiplet. This is due to the fact that the electronic spin, S (or nuclear spin I), has no time to rotate during the collision time (of the order of ρ/v, the mean duration of the collision). This is only true in LS coupling.

3. The Semiclassical Perturbation Approximation (SCP) for Stark-Broadening Studies

We study the case of isolated lines in the impact and complete collision approximations recalled in the preceding section.

Within the semiclassical approximation, the perturbers (electrons or positive ions) are assumed to be classical particles, and they move along a classical path unperturbed by the interactions with the radiating atom. The atom is described by its quantum wave-functions and energy levels. With the perturbation approximation, the atom–perturber interaction is treated by the time-dependent perturbation theory. The long-range approximation will be made.

3.1. The Semiclassical Approximation and the Parametric Representation of the Orbits

For neutral radiating atoms, the trajectory is rectilinear, and for radiating ions, it is a hyperbola. The parametric representation of the trajectory can be found in [19] for the repulsive case and also in [6] for the attractive case and the straight path case. The radiating atom is at the origin, O, of the axes. The quantization axis, Oz, is perpendicular to the collision plane, xOy, and the velocity vector of the perturber is parallel to Ox at time $t = -\infty$. Z_A is the charge of the radiating atom ($Z_A = 0$ for a neutral), Z_P the charge of the perturber ($Z_P = 1$ for an electron), μ the reduced mass of the system atom–perturber, v the relative velocity and ρ the impact parameter.

The coordinates are given in Table 1.

Table 1. Parametric representation of the orbits (trajectories).

	Attractive Hyperbola	**Repulsive Hyperbola**	**Straight Path**
x	$a\,(\varepsilon - \cosh u)$	$a\,(\varepsilon + \cosh u)$	ρ
y	$a\sqrt{\varepsilon^2 - 1}\,\sinh u$	$a\sqrt{\varepsilon^2 - 1}\,\sinh u$	$\rho \sinh u$
t	$\frac{a}{v}\,(\varepsilon\,\sinh u - u)$	$\frac{a}{v}\,(\varepsilon\,\sinh u + u)$	$\frac{\rho}{v}\sinh u$
distance of closest approach	$a(\varepsilon - 1)$	$a(\varepsilon + 1)$	ρ

For radiating ions, $a = e^2 \frac{Z_A Z_P}{\mu v^2}$ is the semi-major axis of the hyperbola, e is the electron charge and $\varepsilon = \left(1 + \frac{\rho^2}{a^2}\right)^{\frac{1}{2}}$ is the eccentricity.

3.2. The Time-Dependent Perturbation Approximation for the Calculation of the S (or T) Matrix

We use the following expression for the S-matrix:

$$S = \mathcal{T}\left(\exp\left(\frac{1}{\mathrm{i}\hbar}\int_{-\infty}^{+\infty} \tilde{V}(t)\,\mathrm{d}t\right)\right) \tag{20}$$

where $\mathcal{T}$ is the chronological operator and $\tilde{V}(t)$ is the atom–perturber interaction potential in interaction representation. Now, we make the second order perturbation theory: we expand the $S-$matrix given

by Equation (20) in multipoles (the so-called Dyson series), and we retain the two first terms of the expansion:

$$S = 1 + \frac{1}{\mathrm{i}\hbar}\int_{-\infty}^{+\infty}\tilde{V}(t)\mathrm{d}t + \frac{1}{\mathrm{i}^2\hbar^2}\int_{-\infty}^{+\infty}\tilde{V}(t)\mathrm{d}t\int_{-\infty}^{t}\tilde{V}(t')\mathrm{d}t' \tag{21}$$

and T follows:

$$T = +\frac{\mathrm{i}}{\hbar}\int_{-\infty}^{+\infty}\tilde{V}(t)\mathrm{d}t + \frac{1}{\hbar^2}\int_{-\infty}^{+\infty}\tilde{V}(t)\mathrm{d}t\int_{-\infty}^{t}\tilde{V}(t')\mathrm{d}t'. \tag{22}$$

3.3. The Atom-Perturber Interaction Potential

We will only study the case of an ideal plasma, which is valid if the Debye length is much larger than the mean distance between perturbers. Hence the atom–perturber interaction V is the electrostatic potential between the N atomic electrons, the nucleus of charge $(Z_A + N)$ and the perturber of charge, Z_P (with $Z_P = -1$ for an electron):

$$V = \frac{(Z_A + N)\, Z_P\, e^2}{r_P} - Z_P\, e^2 \sum_{i=1}^{N}\frac{1}{r_{iP}} \tag{23}$$

where r_P is the distance between the nucleus and the perturber and r_{iP} the distance between the i^{th} atomic electron and the perturber. $Z_A = 0$ for a neutral atom.

Then, $1/r_{iP}$ is expanded into multipolar components. We will only retain the long range part, since we will make the long-range perturbation theory. Penetrating orbits are outside the scope of SCP method and code. The $Y_{\lambda\mu}$ denote the spherical harmonics.

$$V = \frac{Z_A\, Z_P\, e^2}{r_P} - \sum_{\lambda=1}^{\infty}\frac{4\pi\, Z_P\, e^2}{2\lambda+1}\frac{1}{r_P^{\lambda+1}}\sum_{\mu=-\lambda}^{+\lambda}\sum_{i=1}^{N} r_i^{\lambda} Y_{\lambda\mu}(\hat{r}_P) Y^*_{\lambda\mu}(\hat{r}_i). \tag{24}$$

The first term of this expansion is the Coulomb term, which does not play any role in the calculation of the S-matrix, due to its spherical symmetry. The following ones have to be retained: the dipole term $(\lambda = 1)$ and the quadrupole term $(\lambda = 2)$.

3.4. Determination of the T-Matrix Elements Using Equations (22) and (24) and the Coordinates of the Perturber

Thanks to the preceding subsections, we are now able to obtain the semiclassical perturbation expressions of Equations (16) and (17). The $T-$matrix elements, which enter Formula (16), read:

$$\begin{aligned}\langle \alpha_i J_i M_i|T(\rho,v)\,|\alpha_i J_i M_i'\rangle &= \tfrac{\mathrm{i}}{\hbar}\textstyle\int_{-\infty}^{+\infty}\langle \alpha_i J_i M_i|V(\rho,v,\ t)\,|\alpha_i J_i M_i'\rangle\ \mathrm{d}t \\ &+\tfrac{1}{\hbar^2}\textstyle\sum_{\alpha JM}\int_{-\infty}^{+\infty}\langle \alpha_i J_i M_i|V(\rho,v,\ t)\,|\alpha J M\rangle\ \mathrm{e}^{\mathrm{i}\omega_{ij}t}\mathrm{d}t\ \int_{-\infty}^{t}\langle \alpha J M|V(\rho,v,\ t')\,|\alpha_i J_i M_i'\rangle\ \mathrm{e}^{-\mathrm{i}\omega_{ij}t'}\mathrm{d}t'\end{aligned}, \tag{25}$$

where ω_{ij} is the angular frequency difference between the initial i $(\alpha_i J_i)$ level and the perturbing j (αJ) level. We have an analogous expression for the final f $(\alpha_f J_f)$ level.

The first term of Equation (16) is the first direct term, originating from the initial level. It reads:

$$\sum_{M_i} \langle \alpha_i J_i M_i | T(\rho, v) \, | \alpha_i \, J_i \, M_i \rangle = \tfrac{\mathrm{i}}{\hbar} \sum_{M_i} \int_{-\infty}^{+\infty} \langle \alpha_i \, J_i \, M_i | V(\rho, v, t) \, | \alpha_i \, J_i \, M_i \rangle \, \mathrm{d}t$$

$$+ \tfrac{1}{\hbar^2} \sum_{\alpha J M M_i} \int_{-\infty}^{+\infty} \langle \alpha_i \, J_i \, M_i | V(\rho, v, \, t) \, | \alpha J \, M \rangle \, \mathrm{e}^{\mathrm{i}\omega_{ij} t} \mathrm{d}t \int_{-\infty}^{t} \langle \alpha J \, M | V(\rho, v, \, t') \, | \alpha_i \, J_i \, M_i \rangle \, \mathrm{e}^{-\mathrm{i}\omega_{ij} t'} \mathrm{d}t' \tag{26}$$

The second term of Equation (16) is the second direct term, originating from the final level, αJ_f, and has an analogous expression.

The third term of Equation (16) is the interference term.

Then, we use the second order long-range expansion of the interaction potential (Equation (24)). We do not enter the details of the calculations, which can be found in Sahal-Bréchot [6].

We summarize the different steps and only give the resulting formulae in the following:

• The quadrupolar potential is taken into account only for elastic collisions and for inelastic collisions between the fine structure levels of the initial and final levels.

• The fist term of Equation (26) is taken as equal to zero:

−It is exactly equal to zero for the ($\lambda = 1$)-dipolar potential contribution, due to selection rules on the "$3j$" coefficients.

−It is only different from zero for the ($\lambda = 2$)-quadrupolar potential contribution in the case of $J_i \geq 1$ integer numbers, but is neglected.

• The second term of Equation (26) contains quadrupolar and dipolar elements.

• There is no interference terms between dipolar and quadrupolar contributions, which add independently.

• The Debye screening is taken into account by introducing an upper cutoff at the Debye length. The calculations are detailed in [6] for obtaining the $T-$matrix elements and in [7] for the integration over the impact parameters and the choice of the cutoffs.

The full width at half-maximum intensity, W, and the shift, d, of the $i - f$ line can be put under the form [7]:

$$W = N_P \int v f(v) dv \left(\sum_{i' \neq i} \sigma_{ii'}(v) + \sum_{f' \neq f} \sigma_{ff'}(v) + \sigma_{el} \right) \tag{27}$$

Here, the perturbing levels are denoted as i' and f' for simplicity in the writing.

• The inelastic contribution of the upper level, i, is calculated as follows [7]. The dipolar interaction potential is taken into account:

$$\sum_{i' \neq i} \sigma_{ii'}(v) = \frac{1}{2} \pi R_1^2 + \int_{R_1}^{R_D} 2\pi \rho d\rho \sum_{i' \neq i} P_{ii'}(\rho, v) \tag{28}$$

$$P_{ii'}(\rho, v) = \frac{1}{\hbar^2} \left| \int_{-\infty}^{+\infty} V_{ii'} \exp \left(-\frac{\mathrm{i}}{\hbar} \Delta E_{ii'} \, t \right) \right|^2 \tag{29}$$

with $\Delta E_{ii'} = \hbar\omega_{ii'}$.

The upper cutoff, R_D, is the Debye radius. The lower cutoff, R_1, is chosen as in [7,14]:

$$\sum_{i' \neq i} P_{ii'}(\rho,\, v) = \frac{1}{2}$$

or, in the case of electron collisions:

$$\sum_{i' \neq i} \sigma_{ii'}(v) = \int_{\min(\langle r_i \rangle, \langle r_i{}' \rangle)}^{R_D} 2\pi\rho d\rho \sum_{i' \neq i} P_{ii'}(\rho, v) \tag{30}$$

where $\langle r_i \rangle$ is the mean radius of the i level and $\langle r_i{}' \rangle$ is the mean radius of the i' level. An hydrogenic approximation is sufficient for calculating these mean radii, and we retain as in [14] the smallest result between the one of Equation (29) and the one of Equation (30). This minimizes [14] the role of close collisions, which are considered as overestimated by the perturbation theory.

In the case of collisions with positive ions (*cf.* [20]), we retain the smallest between the result of Equation (28) and of the following one:

$$\sum_{i' \neq i} \sigma_{ii'}(v) = \pi \langle r_i \rangle^2 P_{ii'}\left(\langle r_i \rangle, v\right) + \int_{\langle r_i \rangle}^{R_D} 2\pi\,\rho \mathrm{d}\rho \sum_{i' \neq i} P_{ii'}(\rho, v) \tag{31}$$

The inelastic contribution from the lower level, f, is calculated in the same way.

• The contribution of elastic collisions, σ_{el}, is calculated as follows:

$$\sigma_{el} = 2\pi R_2^2 + \int_{R_2}^{R_D} 2\pi\rho d\rho \sin^2\varphi + \sigma_r \tag{32}$$

with:

$$\varphi = (\varphi_p^2 + \varphi_q^2)^{\frac{1}{2}} \tag{33}$$

and:

$$\varphi_p = \sum_{i' \neq i} \varphi_{ii'} - \sum_{f' \neq f} \varphi_{ff'} \tag{34}$$

The phase shifts, φ_p and φ_q, are due, respectively, to the dipolar potential (the polarization potential in the adiabatic approximation) and to the quadrupolar potential. The contribution of the dipolar interaction to the width is often denoted as the quadratic contribution. Their expressions will be detailed hereafter. The lower cutoff, R_2, is chosen as $\varphi(R_2, v) = 1$ [7]. The interference term is taken into account in φ_p and φ_q.

Here, σ_r is the contribution of the Feshbach resonances [9], which concerns only ionized radiating atoms colliding with electrons. It is an extrapolation of the excitation collision strengths (and not the cross-sections) under the threshold by means of the semiclassical limit of the Gailitis approximation (see [9] for details of the calculations).

• The shift, d, is given by (the dipolar interaction potential is the only one to be taken into account):

$$d = N_P \int v f(v) dv \int_{R_3}^{R_D} 2\pi\rho d\rho \sin(2\varphi_p) \tag{35}$$

The cutoff, R_3 [7], is chosen as $2\varphi_p(\rho, v) = 1$. There is no strong collision term for the shift.

3.5. Expressions of $P_{ii'}(\rho, v)$, $P_{ff'}(\rho, v)$, $\varphi_p(\rho, v)$, $\varphi_q(\rho, v)$, Symmetrization and Some Asymptotic Limits

We use CGS units, but we will often use atomic units ($\hbar = 1$, $e = 1$, $m_e = 1$, and thus, $a_0 = 1$, $I_H = 1/2$):
$a_0 = \frac{\hbar^2}{m_e e^2}$ is the first Bohr orbit radius, m_e is the electron mass and e the electron charge. $I_H = \frac{m_e e^4}{2\hbar^2}$is the ionization energy of hydrogen (1 Rydberg).

3.5.1. Case of Neutral Atoms (Straight Path)

Contribution of the dipolar interaction: expressions of the transition probabilities, of the inelastic cross-sections and of φ_p

$$\frac{1}{2}P_{ii'}(\rho, v) + 2\,\mathrm{i}\varphi_{ii'}\,(\rho, v) = \frac{a_0^2}{\rho^2}\frac{2\,I_H^2}{E\,\Delta E_{ii'}} f_{ii'}\frac{\mu}{m_e}\,Z_P^2\,\left(A(z) + \mathrm{i}B(z)\right) \tag{36}$$

$z = \frac{\rho\,\Delta E_{ii'}}{\hbar\,v}$, $f_{ii'}$ is the oscillator strength of the (ii') transition, and $E = \frac{1}{2}\mu\,v^2$ is the incident kinetic energy of the perturber.

$$A(z) + \mathrm{i}B(z) = \frac{1}{2}\int_{-\infty}^{+\infty}\mathrm{d}u\int_{-\infty}^{u}\mathrm{d}u'\left(\frac{1+\sinh u\ \ \sinh u'}{\cosh^2 u\ \cosh^2 u'}\exp\left(\mathrm{i}z\left(\sinh u - \sinh u'\right)\right)\right) \tag{37}$$

$A(z)$ and $B(z)$ are connected together by the Hilbert transform:

$$B(z) = \tfrac{1}{\pi}\mathrm{pv}\int_{-\infty}^{+\infty}\mathrm{d}z'\tfrac{A(z')}{z-z'}$$

$$A(z) = \tfrac{1}{\pi}\mathrm{pv}\int_{-\infty}^{+\infty}\mathrm{d}z'\tfrac{B(z')}{z-z'}$$

where pv denotes the Cauchy principal value.
$A(z)$ can be expressed by means of the modified Bessel functions, K_0 and K_1 [14]:

$$A(z) = z^2\left(|K_0(z)|^2 + |K_1(z)|^2\right) \tag{38}$$

and the expression of $B(z)$ was obtained by [21]:

$$B(z) = \pi\,z^2\left(|K_0(z)|\,|I_0(z)| - |K_1(z)|\,|I_1(z)|\right). \tag{39}$$

Then, we integrate over the impact parameter for obtaining the inelastic, ii', contribution:

$$\int_{R_1}^{R_D} 2\pi\rho\,\mathrm{d}\rho\ \ P_{ii'}(\rho, v) = \pi a_0^2\,\frac{8\,I_H^2}{E\,\Delta E_{ii'}}\,f_{ii'}\frac{\mu}{m_e}\,Z_P^2\,\left(a(z_D) - a(z_1)\right) \tag{40}$$

with [14]:

$$a(z) = z\ |K_1(z)|\,K_0(z).$$

Symmetrization

We now introduce the symmetrization of the transition probabilities and cross-sections, in order to satisfy the reciprocity relations [14]. We replace E by E_{sym} and z by z_{sym}:

$$E_{sym} = \frac{1}{2}\left(2E - \Delta E_{ii'}\right) \tag{41}$$

$$z_{sym} = \frac{\rho}{a_0}\sqrt{\frac{\mu}{m_e}}\sqrt{\frac{E}{I_H}}\frac{\Delta E_{ii'}}{2E - \Delta E_{ii'}}. \tag{42}$$

Remark concerning the shift

Note that in the SCP method and computer code, we calculate the shift with Equation (35). Thus, the integration over the impact parameter is not analytical. However, we have also calculated the shift with the more usual formula, where the $b(z)$ function [21] appears:

$$\int_{R_4}^{R_D} 2\pi\rho\,\mathrm{d}\rho\; 2\varphi_{ii'}(\rho, v) = \pi a_0^2 \frac{4\,I_H^2}{E\,\Delta E_{ii'}}\, f_{ii'}\frac{\mu}{m_e}\, Z_P^2\, \left(b(z_D) - b(z_4)\right) \tag{43}$$

$$b(z) = \frac{\pi}{2} - \pi\, z\, K_0(z)\, I_1(z) \tag{44}$$

In that case, we have chosen the lower cutoff, R_4, as equal to $\frac{1}{2}\left(\langle r_i\rangle + \langle r_f\rangle\right)$ where $\langle r_i\rangle$ is the mean radius of the i level and $\langle r_f\rangle$ the mean radius of the f level. In fact, the obtained results are quite sensitive to the cutoff, and we have preferred our method of calculation given by Equation (35). Therefore, our shift results with the $b(z)$ function appear neither in our publications nor in the STARK-B database.

Asymptotic limits and series expansions of $A(z)$, $a(z)$, $B(z)$

The asymptotic limits of $A(z)$, $B(z)$ and $a(z)$ are recalled hereafter, because they are useful for understanding some systematic trends: At high energies (or very small ΔE):

$A(z) \to 1$, $\frac{\partial A}{\partial z} \to$ zero,

$a(z) \to \ln\left(\frac{2}{\gamma z}\right)$ and

$B(z) \to 0$ and $\frac{\partial B}{\partial z} \to$ zero.

$\gamma = \exp C$ and $C = 0.5772156649$ is the Euler constant.

At low energies (or high ΔE): $A(z) \to \pi\, z \exp(-2z)$, $B(z) \to \pi/4z + 9\pi/32z^2 + ...$ and $a(z) \to \frac{\pi}{2}\exp(-2z)$.

In fact, at low energies, the Lindholm limit due to a polarization potential of the phase shift, φ_p, is obtained (*cf.* [22]). The limit ($\beta \to 0$) is $\varphi_p = \varphi_i - \varphi_f$, with:

$$\varphi_i = \sum_{i' \neq i} \frac{\pi}{2} Z_P^2 \left(\frac{a_0}{\rho}\right)^3 \sqrt{\frac{I_H}{E}}\sqrt{\frac{\mu}{m_e}} f_{ii'} \left(\frac{I_H}{\Delta E_{ii'}}\right)$$

with an analogous expression for φ_f. *Contribution of the quadrupolar interaction: expression of φ_q*

This only concerns the elastic term of the width (*cf.* above). The contribution of the inelastic transitions between fine structure levels of the initial and final level (if any) are included in the elastic term. The details of the calculations are given in [6], in [8] for the B_i, B_f, B_{if} angular coefficients of complex atoms and in [13] for still more complex atoms. We have [6]:

$$\varphi_q^2 = \left[\left(B_i\left\langle r_i^2\right\rangle\right)^2 + \left(B_f\left\langle r_f^2\right\rangle\right)^2 - B_{if}\left\langle r_i^2\right\rangle\left\langle r_f^2\right\rangle\right] Z_P^2 \frac{\mu}{m_e}\frac{a_0^4}{\rho^4}\frac{I_H}{E} \tag{45}$$

In the SCP computer code, the calculations of the Bessel functions use the Fortran library of [23]. The integration over the impact parameter of the elastic part of the width and of the shift use Gauss

integration techniques and Gauss–Laguerre integration techniques for the integration over the Maxwell distribution of velocities. The Gauss–Laguerre technique is not suitable for the inelastic part, because at high energies, the inelastic dipolar cross-sections decrease as $(\ln E)/E$. A trapezoidal method with an increasing exponential step is used; it is suitable and accurate.

3.5.2. Case of Ionized Atoms (Hyperbolic Path)

Contribution of the dipolar interaction: expressions of the transition probabilities, of the inelastic cross-sections and of φ_p

We define:

$$\xi = \frac{a\,\Delta E_{ii'}}{\hbar v} = \frac{1}{2} Z_A\, Z_P \sqrt{\frac{\mu}{m_e}} \frac{\Delta E_{ii'}}{I_H} \left(\frac{I_H}{E}\right)^{\frac{3}{2}}$$

and we obtain:

$$\frac{1}{2} P_{ii'}(\varepsilon, v) + 2\,\mathrm{i}\,\varphi_{ii'}(\varepsilon, v) = \frac{a_0^2}{(a\varepsilon)^2} \frac{2\,I_H^2}{E\,\Delta E_{ii'}} f_{ii'} \frac{\mu}{m_e}\, Z_P^2\, \left(A(\xi, \varepsilon) + \mathrm{i}B(\xi, \varepsilon)\right) \tag{46}$$

$$A(\xi, \varepsilon) = (\xi\varepsilon)^2 \exp(\pm\pi\xi) \left(\left|K_{\mathrm{i}\xi}(\xi\varepsilon)\right|^2 + \frac{\varepsilon^2 - 1}{\varepsilon^2} \left|K'_{\mathrm{i}\xi}(\xi\varepsilon)\right|^2 \right) \tag{47}$$

where $\pm$ means $+$ for the attractive case and $-$ for the repulsive case.

We recognize the Bessel functions of imaginary order $\mathrm{i}\xi$ and real argument $\xi\varepsilon$:

$$\begin{array}{l} K_{\mathrm{i}\xi}(\xi\,\varepsilon) = \int_0^\infty \mathrm{e}^{-\xi\,\varepsilon\,\cosh u} \cos\xi u\ \mathrm{d}u \\ K'_{\mathrm{i}\xi}(\xi\,\varepsilon) = \int_0^\infty \mathrm{e}^{-\xi\,\varepsilon\,\cosh u} \cos\xi u\ \cosh u\ \mathrm{d}u \end{array} \tag{48}$$

As for the straight path case, $A(\xi, \varepsilon)$ and $B(\xi, \varepsilon)$ are connected together by the Hilbert transform, but now, the variable is ξ:

$$B(\xi,\, \varepsilon) = \frac{1}{\pi} \mathrm{pv} \int_{-\infty}^{+\infty} \mathrm{d}\xi' \frac{A(\xi',\, \varepsilon)}{\xi - \xi'} \tag{49}$$

Contrary to the straight path case, we do not know any other analytical formula for $B(\xi, \varepsilon)$. Therefore, it will be calculated numerically by using asymptotic formulae, which will be given hereafter.

For the attractive case, $B(\xi, \varepsilon)$ has also been calculated by use of the Hilbert transform when asymptotic formulae are not adequate. However, Equation (49) is not suitable for numerical calculations. In the SCP computer code, the dispersion relation has been used:

$$B(\xi,\, \varepsilon) = \frac{1}{\pi} \int_{0+}^{+\infty} \mathrm{d}\xi' \frac{A(\xi - \xi',\, \varepsilon) - A(\xi + \xi',\, \varepsilon)}{\xi'} \tag{50}$$

and also the second imaginary term of the Dyson series:

$$\begin{array}{l} B(\xi,\, \varepsilon) = \frac{1}{2} \int_{-\infty}^{+\infty} \mathrm{d}u \int_{-\infty}^{u} \mathrm{d}u' \left[\sin\left[\xi\,(\varepsilon(\sinh u - \sinh u') - (u - u')\right]\right. \\ \left. \times\ \frac{\varepsilon^2 + (\varepsilon^2 - 1)\sinh u \sinh u' + \cosh u \cosh u' - \varepsilon(\cosh u + \cosh u')}{(\varepsilon \cosh u - 1)^2 (\varepsilon \cosh u' - 1)^2} \right] \end{array} \tag{51}$$

The integration over the impact parameter of the transition probability, $P_{ii'}(\xi,\varepsilon)$, has an analytic solution:

$$\int_{R_1}^{R_D} 2\pi\rho \, \mathrm{d}\rho \sum_{i'\neq i} P_{ii'}(\rho,v) = 8\pi a_0^2 \frac{2\, I_H^2}{E\, \Delta E_{ii'}} f_{ii'} \frac{\mu}{m_e} Z_P^2 \, (a(\xi,\varepsilon_D) - a(\xi,\varepsilon_1))$$

with:

$$a(\xi,\varepsilon) = \exp(\pm\pi\xi) \; \xi\varepsilon \, K_{\mathrm{i}\xi}(\xi\varepsilon) \, K'_{\mathrm{i}\xi}(\xi\varepsilon) \tag{52}$$

where $\pm$ means $+$ for the attractive case and $-$ for the repulsive case.

Sample graphs of the $A(\xi,\varepsilon)$, $a(\xi,\varepsilon)$ and $B(\xi,\varepsilon)$ functions are displayed in [5,24,25].

Symmetrization of the transition probabilities and cross-sections

As for the straight path case, the transition probabilities and cross-sections are also symmetrized [7,19,24].

a and ξ become a_{sym} and ξ_{sym}, with $E_i = E$, $E'_i = E_i + \Delta E_{ii'}$:

$a_{sym} = a_0 \, I_H \frac{Z_A \, Z_P}{\sqrt{E_i \, E_{i'}}}$ and

$\xi_{sym} = Z_A \, Z_P \sqrt{\frac{\mu}{m_e}} \left(\sqrt{\frac{I_H}{E_i}} - \sqrt{\frac{I_H}{E_{i'}}} \right)$.

Asymptotic and series expansions for A, a and B, used in the computer code

(1) First, we recall that:

$$A\,(0,\ \varepsilon) = 1$$
$$\frac{\partial A}{\partial \xi}\,(0^+,\ \varepsilon) = \pm\pi$$

with $\pm$: $+$ for the attractive case and $-$ for the repulsive case.

$$B\,(0,\ \varepsilon) = 1$$
$$\frac{\partial B}{\partial \xi}\,(0^+,\ \varepsilon) = \mp\infty$$

with $\mp$: $-$ for the attractive case and $+$ for the repulsive case.

(2) At high energies, E, or small $\Delta E_{ii'}$, $\xi \to$ zero, one obtains:

$$a(\xi,\ \delta) = (1 \pm \pi\xi) \ln\left(\frac{2}{\gamma+\delta}\right) \tag{53}$$

with $\delta = \xi(\varepsilon - 1)$ and with $\gamma = \mathrm{e}^C$. C is the Euler constant. We have used this asymptotic expression for calculating $A(\xi,\delta)$ and $a(\xi,\delta)$ for $\xi < 0.1$ and for $\delta < 0.025$.

At very high energies, the Coulomb attraction (or repulsion) becomes weak; the contribution of high impact parameters predominates, $\xi\varepsilon \to \rho$, and the straight path case is recovered.

(3) For high ξ and high $\xi\varepsilon$, the following asymptotic expansion—valid for order and argument both high and nearly equal ([26] p. 245 and [27] p. 88, [28], such as $\delta = \xi\varepsilon - \xi = o(\xi\varepsilon)^{1/3}$)—has been used:

$$\begin{aligned} K_{i\xi}(\xi\varepsilon) &= \tfrac{1}{3}e^{-\frac{\pi\xi}{2}} \sum_{m=0}^{\infty} \sin\left(\tfrac{(m+1)\pi}{3}\right) \Gamma\left(\tfrac{m+1}{3}\right) \left(\tfrac{\xi\varepsilon}{6}\right)^{-\frac{m+1}{3}} A_m \\ K'_{i\xi}(\xi\varepsilon) &= \tfrac{1}{6}e^{-\frac{\pi\xi}{2}} \sum_{m=0}^{\infty} \sin\left(\tfrac{(m+1)\pi}{3}\right) \Gamma\left(\tfrac{m+1}{3}\right) \left(\tfrac{\xi\varepsilon}{6}\right)^{-\frac{m+1}{3}} A'_m \\ &+ \tfrac{1}{3}e^{-\frac{\pi\xi}{2}} \sum_{m=0}^{\infty} \sin\left(\tfrac{(m+1)\pi}{3}\right) \Gamma\left(\tfrac{m+1}{3}\right) \left(\tfrac{\xi\varepsilon}{6}\right)^{-\frac{m+4}{3}} \left(-\tfrac{m+1}{18}\right) A_m \end{aligned} \quad (54)$$

We have expanded the series up to $m = 4$ [28] in the SCP code. The A_m and A'_m coefficients are given in Table 2.

Table 2. Values of the coefficients A_m and A'_m in Equation (54) [28].

m	A_m	A'_m
0	1	0
1	$-\delta$	-2
2	$\delta^2/2 + 1/20$	2δ
3	$-\delta^3/6 - \delta/15$	$-\delta^2 - 2/15$
4	$\delta^4/24 + \delta^2/24 + 1/280$	$\delta^3/3 + \delta/6$

Note that there is a typo in [28]. Therefore, the correct formulae are:

$$\begin{aligned} K_{i\xi}(\xi\varepsilon) &= \tfrac{\sqrt{3}}{6}e^{-\frac{\pi\xi}{2}} \left[\Gamma\left(\tfrac{1}{3}\right)\left(\tfrac{6}{\xi\varepsilon}\right)^{\frac{1}{3}} - \Gamma\left(\tfrac{2}{3}\right)\left(\tfrac{6}{\xi\varepsilon}\right)^{\frac{2}{3}}\delta + \Gamma\left(\tfrac{4}{3}\right)\left(\tfrac{6}{\xi\varepsilon}\right)^{\frac{4}{3}}\tfrac{\delta}{3}\left(0.5\delta^2 + 0.2\right)\right. \\ &\left. - \Gamma\left(\tfrac{5}{3}\right)\left(\tfrac{6}{\xi\varepsilon}\right)^{\frac{5}{3}}\left(\tfrac{\delta^4+\delta^2}{3} + \tfrac{1}{35}\right)\right] \\ K'_{i\xi}(\xi\varepsilon) &= \tfrac{\sqrt{3}}{12}e^{-\frac{\pi\xi}{2}}\left(\tfrac{6}{\xi\varepsilon}\right)^{\frac{2}{3}}\left[2\,\Gamma\left(\tfrac{2}{3}\right) + \left(\tfrac{6}{\xi\varepsilon}\right)^{\frac{2}{3}}\left(-\Gamma\left(\tfrac{4}{3}\right)\left(\delta^2 + \tfrac{2}{15}\right)\right)\right. \\ &\left. + \tfrac{1}{9}\Gamma\left(\tfrac{1}{3}\right) + \left(\tfrac{6}{\xi\varepsilon}\right)\left(\Gamma\left(\tfrac{5}{3}\right)\tfrac{\delta}{6}\left(1+\delta^2\right) - \tfrac{2}{9}\Gamma\left(\tfrac{2}{3}\right)\delta\right)\right] \end{aligned} \quad (55)$$

(4) When $\varepsilon \to \infty$ (or $\delta \to \infty$), we have used the expansion ([26] p. 202):

$$\begin{aligned} K_{i\xi}(\xi\varepsilon) &= \left(\tfrac{\pi}{2\xi\varepsilon}\right)^{\frac{1}{2}} e^{-\xi\varepsilon}\left[\sum_{k=0}^{\infty} \frac{\left(-4\xi^2-1\right)\left(-4\xi^2-9\right)\ldots\left(-4\xi^2-(2k-1)^2\right)}{k!\,(8\xi\varepsilon)^k}\right] \\ K'_{i\xi}(\xi\varepsilon) &= -\left(\tfrac{\pi}{2\xi\varepsilon}\right)^{\frac{1}{2}} e^{-\xi\varepsilon}\left[\sum_{k=0}^{\infty} \frac{\left(-4\xi^2+16k^2-1\right)\ldots\left(-4\xi^2-(2\,(2k-1)-1)^2\right)}{(2k)!\;(8\xi\varepsilon)^k}\right. \\ &\left. + \sum_{k=0}^{\infty} \frac{\left(-4\xi^2+4(2k+1)^2-1\right)\ldots\left(-4\xi^2-(4k-1))^2\right)}{(2k+1)!\;(8\xi\varepsilon)^{2k+1}}\right] \end{aligned} \quad (56)$$

We have used this expansion for calculating $A(\xi,\delta)$ and $a(\xi,\delta)$ for $\xi < 10$ and $\delta > 90$.

(5) Beyond the validity of these above expansions, the $K_{i\xi}(\xi,\delta)$ and $K'_{i\xi}(\xi,\delta)$ functions have been calculated with an unpublished Fortran subroutine developed in [24]. The $A(\xi,\delta)$ and $a(\xi,\delta)$ follow.

(6) Asymptotic expansions for $B(\xi,\varepsilon)$ for the attractive case (collisions with electrons).

We have used two expansions. The first one is valid for high values of ξ, and the first two terms were calculated by [6]. We have added the third term of the expansion in the numerical SCP code. It reads:

$$\begin{aligned} B(\xi,\varepsilon) = {} & \tfrac{\varepsilon^2}{2\xi(\varepsilon^2-1)^2}\left[3+(2+\varepsilon^2)\,\tfrac{\pi-\arccos\left(\frac{1}{\varepsilon}\right)}{\sqrt{\varepsilon^2-1}}\right] \\ & + \tfrac{\varepsilon^2}{16\,\xi^3(\varepsilon^2-1)^5}\left[\tfrac{124+592\,\varepsilon^2+229\varepsilon^4}{3}+(16+152\varepsilon^2+138\varepsilon^4+9\varepsilon^6)\,\tfrac{\pi-\arccos\left(\frac{1}{\varepsilon}\right)}{\sqrt{\varepsilon^2-1}}\right] \\ & + \tfrac{\varepsilon^2}{256\,\xi^5(\varepsilon^2-1)^8}\left[\tfrac{4576+144160\,\varepsilon^2+539524\varepsilon^4+392088\varepsilon^6+45777\varepsilon^8}{5}\right. \\ & \left. + (256+13952\varepsilon^2+82752\varepsilon^4+101600\varepsilon^6+25990\,\varepsilon^8+675\,\varepsilon^{10})\,\tfrac{\pi-\arccos\left(\frac{1}{\varepsilon}\right)}{\sqrt{\varepsilon^2-1}}\right] \end{aligned} \tag{57}$$

For $\varepsilon < 1.01$, we have used the expansion derived by [29], and we have limited it to the first two terms in the SCP code. It reads:

$$B\left(\xi,\,\varepsilon\right) = \sqrt{3\pi}\,\varepsilon^{\frac{3}{2}}\,\xi^{\frac{2}{3}}\left(-0.940+2.228\left(\varepsilon-1\right)\xi^{\frac{2}{3}}\right). \tag{58}$$

For high values of ξ and high values of ε, we have used the asymptotic form:

$$B\left(\xi,\,\varepsilon\right) = \frac{3\pi\,\varepsilon^2}{2\xi(\varepsilon^2-1)^{\frac{5}{2}}} = \frac{2\pi a^5}{3\,\xi\,\rho^5}. \tag{59}$$

(7) Beyond the validity of these expansions, $B(\xi,\varepsilon)$ has been calculated by means of a numerical integration of the Hilbert transform (Equation (50)) or by a numerical integration of the second imaginary term of the Dyson series (Equation (52)).

(8) Asymptotic expansions for $B(\xi,\varepsilon)$ for the repulsive case (collisions with positive ions).

Due to the mass effect, ξ is always high in typical conditions for Stark broadening studies. Therefore, an expansion valid for high values of ξ is sufficient and has been introduced in the SCP computer code. It reads [6]:

$$B\left(\xi,\,\varepsilon\right) = \frac{\varepsilon^2}{2\xi\left(\varepsilon^2-1\right)}\left(\frac{2+\varepsilon^2}{\sqrt{\varepsilon^2-1}}\arccos\left(\frac{1}{\varepsilon}\right)-3\right)+(...)\,. \tag{60}$$

If in addition, $\varepsilon \to 1$:

$$B\left(\xi,\,\varepsilon\right) = \frac{\varepsilon^2}{2\xi}\left(\frac{2}{15}-\frac{4}{35}\left(\varepsilon^2-1\right)+\frac{2}{21}\left(\varepsilon^2-1\right)^2-\frac{8}{99}\left(\varepsilon^2-1\right)^3+...\right). \tag{61}$$

Contribution of the quadrupolar interaction: expression of φ_q for radiating ions

After an elementary calculation, one obtains [6]:

$$\begin{aligned} \varphi_q^2 = {} & \left[\left(B_i\left\langle r_i^2\right\rangle\right)^2+\left(B_f\left\langle r_f^2\right\rangle\right)^2-B_{if}\left\langle r_i^2\right\rangle\left\langle r_f^2\right\rangle\right]\tfrac{\mu}{m_e}\tfrac{Z_P^2}{(a^2\varepsilon^2)^2}\tfrac{I_H}{E} \\ & \times\left[\tfrac{1}{4}+\tfrac{3\,\varepsilon^4}{4(\varepsilon^2-1)^2}\left(1+\tfrac{\mp\pi+2\arcsin\left(\frac{1}{\varepsilon}\right)}{2\sqrt{\varepsilon^2-1}}\right)\right] \end{aligned} \tag{62}$$

where $\mp$ means $+$ for the attractive case and $-$ for the repulsive case.

At high eccentricities or high energies (as expected), we recover the straight path limit. At low energies and small eccentricities, by using the series expansion of $\arcsin 1/\varepsilon$, we obtain [6] the asymptotic phase shift found in [22] for electron collisions.

4. Results and Discussion

4.1. Validity of the Impact Approximation

The impact approximation is at the basis of the SCP method. Its validity is checked in all of the calculations for every line, every temperature and every density by using Equation (6).

The collision volume is calculated by writing $W = N_P v_{typ} \rho_{typ}^2$, where W is the calculated width, N_P the density of the perturbers and v_{typ} is the mean relative velocity. Thus, ρ_{typ} can be derived. One of the outputs of the code is $N_P V$, where $V = \rho_{typ}^3$ is the collision volume.

We give, in the following (Tables 3–6), two examples. Table 3 (electron collisions) and Table 4 (proton collisions) concern the case of Ne VIII $3s - 3p$ at 10^{19} cm^{-3}. The data are taken from the cases studied at the Spectral Line Shapes in Plasmas workshop (April, 2012). Table 5 (electron collisions) and Table 6 (proton collisions) concern the case of Li I $2s - 2p$ at 10^{16} cm^{-3}.

The results for $N_P V$ show that the impact approximation is valid both for electron and proton colliders in these two cases.

In the STARK-B database, the values of the widths and shifts are provided in the tables, except when $N_P V > 0.5$, where the cells are empty and marked with an asterisk preceding the cell. Widths and shifts values for $0.1 < N_P V < 0.5$ are given and marked by an asterisk in the cell preceding the value.

The format of the data of Tables 3–6 is in ASCII. Hence, E + 05 means $\times 10^5$, and so on.

Table 3. Results of the SCP code for Ne VIII $3s - 3p$, electron collisions. Angular frequency units, density $N_P = 10^{19}$ cm^{-3}, temperatures T in Kelvin.

T	0.580E + 05	0.174E + 06	0.580E + 06
$N_P V$	0.579E − 02	0.121E − 02	0.238E − 03
Full width at half maximum	0.105E + 14	0.639E + 13	0.394E + 13
Strong collisions contribution	0.347E + 13	0.202E + 13	0.112E + 13
Inelastic collision contribution from the upper level	0.233E + 13	0.176E + 13	0.125E + 13
Inelastic collision contribution from the lower level	0.687E + 12	0.942E + 12	0.801E + 12
Feshbach resonances contribution from the upper level	0.431E + 12	0.915E + 11	0.156E + 11
Feshbach resonances contribution from the lower level	0.151E + 13	0.409E + 12	0.767E + 11
Elastic collisions contribution (polarization + quadrupole)	0.744E + 13	0.369E + 13	0.189E + 13
Elastic collisions contributions (without quadrupole)	0.435E + 11	0.202E + 11	0.799E + 10

Table 4. Results of the SCP code for Ne VIII $3s - 3p$, proton collisions. Angular frequency units, density $N_P = 10^{19}$ cm^{-3}, temperatures T in Kelvin.

T	$0.580\mathrm{E}+05$	$0.174\mathrm{E}+06$	$0.580\mathrm{E}+06$
$N_P V$	$0.205\mathrm{E}-03$	$0.918\mathrm{E}-03$	$0.183\mathrm{E}-02$
Full width at half maximum	$0.269\mathrm{E}+11$	$0.126\mathrm{E}+12$	$0.394\mathrm{E}+13$
Strong collisions contribution	$0.383\mathrm{E}+04$	$0.253\mathrm{E}+09$	$0.204\mathrm{E}+11$
Inelastic collision contribution from the upper level	$0.489\mathrm{E}+05$	$0.557\mathrm{E}+09$	$0.310\mathrm{E}+11$
Inelastic collision contribution from the lower level	$0.511\mathrm{E}-02$	$0.231\mathrm{E}+06$	$0.861\mathrm{E}+09$
Elastic collisions contribution (polarization + quadrupole)	$0.269\mathrm{E}+11$	$0.126\mathrm{E}+12$	$0.334\mathrm{E}+12$
Elastic collisions contribution (without quadrupole)	$0.607\mathrm{E}+09$	$0.184\mathrm{E}+11$	$0.138\mathrm{E}+12$

Table 5. Results of the SCP code for Li I $2s - 2p$, electron collisions. Angular frequency units, density $N_P = 10^{16}$ cm^{-3}, temperatures T in Kelvin.

T	$5,000$	$10,000$	$20,000$
$N_P V$	$0.328\mathrm{E}-04$	$0.221\mathrm{E}-04$	$0.186\mathrm{E}-04$
Full width at half maximum	$0.976\mathrm{E}+10$	$0.106\mathrm{E}+11$	$0.134\mathrm{E}+11$
Strong collisions contribution	$0.583\mathrm{E}+10$	$0.603\mathrm{E}+10$	$0.721\mathrm{E}+10$
Inelastic collision contribution from the upper level	$0.445\mathrm{E}+10$	$0.461\mathrm{E}+10$	$0.567\mathrm{E}+10$
Inelastic collision contribution from the lower level	$0.963\mathrm{E}+08$	$0.827\mathrm{E}+09$	$0.267\mathrm{E}+10$
Elastic collisions contribution (polarization + quadrupole)	$0.522\mathrm{E}+10$	$0.518\mathrm{E}+10$	$0.502\mathrm{E}+10$
Elastic collisions contribution (without quadrupole)	$0.252\mathrm{E}+10$	$0.189\mathrm{E}+10$	$0.113\mathrm{E}+10$

Table 6. Results of the SCP code for Li I $2s - 2p$, proton collisions. Angular frequency units, density $N_P = 10^{16}$ cm^{-3}, temperatures T in Kelvin.

T	$5,000$	$10,000$	$20,000$
$N_P V$	$0.281\mathrm{E}-02$	$0.167\mathrm{E}-02$	$0.998\mathrm{E}-03$
Full width at half maximum	$0.471\mathrm{E}+10$	$0.472\mathrm{E}+10$	$0.472\mathrm{E}+10$
Strong collisions contribution	$0.220\mathrm{E}+10$	$0.220\mathrm{E}+10$	$0.221\mathrm{E}+10$
Inelastic collision contribution from the upper level	$0.206\mathrm{E}+01$	$0.113\mathrm{E}+01$	$0.602\mathrm{E}+02$
Inelastic collision contribution from the lower level	$0.228\mathrm{E}-06$	$0.897\mathrm{E}-02$	$0.200\mathrm{E}+02$
Elastic collisions contribution (polarization + quadrupole)	$0.471\mathrm{E}+10$	$0.472\mathrm{E}+10$	$0.473\mathrm{E}+10$
Elastic collisions contribution (without quadrupole)	$0.789\mathrm{E}+09$	$0.885\mathrm{E}+09$	$0.994\mathrm{E}+09$

In the wings, $\Delta\omega$ being the detuning in angular frequency units, the validity condition of the generalized impact approximation becomes $\tau\ \Delta\omega << 1$. Therefore, if we approach the limit of validity of the impact approximation ($0.1 < N_P V < 0.5$), the impact approximation becomes invalid in the wings. This can be the case of collisions with ions at high densities. However, the contribution of ion collisions is most often weaker than the contribution of electron collisions (about 10%), and a rough accuracy for the contribution of ion collisions is generally sufficient. Of course, exceptions exist, which

arise when some perturbing levels are very close to the upper ones: see below and [30], as well as the explanation given in [31]).

Concerning isolated lines perturbed by electron colliders, the impact approximation is quite always valid, due to the high velocity of these light particles. The only exceptions concern radiating ions at very high densities, which can occur in laser plasmas, for instance.

Besides, it is interesting to recall that hydrogen lines arising from low levels (Balmer lines, for instance), which are not isolated, can be treated within the impact approximation at low densities typical of stellar atmospheres and of some laboratory plasmas: in [32], it was shown that the profile of Hα is Lorentzian in the central part of the profile. A good agreement, for collisions with electrons and protons, as well, was obtained between the impact model and the MMM (model microfield method) one at $N_P = 10^{13}$ cm^{-3} and $T = 5,000$ K and $10,000$ K.

4.2. Validity of the Isolated Line Approximation

At high densities or for lines arising from high levels, the electron impact width can be comparable to the separation, $\Delta E(nl, nl \pm 1)$, between the perturbing energy levels and the initial or final level: the corresponding levels become degenerate, and the isolated line approximation is no longer valid. In order to check the validity of this approximation, we have defined a parameter, C, in [10], which is given in the STARK-B database and the corresponding articles.

4.3. Comparisons of the Different Contributions

An extensive discussion concerning comparisons of the different contributions can be found in [31]. Tables 3–6 give the different contributions to the full width for the two cases cited.

4.3.1. Electron Collisions

The contribution of strong collisions is generally less important for radiating ions than for neutrals. This is due to the Coulomb attraction. The contribution of strong collisions decreases when the energy (or temperature) increases, as expected. Generally, inelastic collisions predominate at high energies and elastic ones at low energies.

Concerning inelastic collisions, the contribution of high impact parameters becomes very important when some perturbing levels are close to the upper one (or to the lower one) or when the energy (or temperature) is high. Then, the SCP method is the most accurate. In addition, one can notice that the summation over the incident electron orbital l-quantum numbers for obtaining cross-sections in quantum methods no longer works if l is too high (l about 30 for S VII). Therefore, the summation is generally completed by using the Born, or the Bethe, or the Coulomb–Bethe approximation (*cf.*, for instance, [33]).

For elastic collisions, the contribution of the quadrupolar interaction is never negligible in these two cases. The contribution of small impact parameters is most often predominant. The contribution of elastic collisions can be negligible when some perturbing levels are very close to the upper ones [31].

In addition, a detailed comparison between close-coupling and SCP calculations is given in [34] for the electron impact broadening of the Li I resonance line. In particular, it is shown that the close-coupling and SCP calculations converge at $l = 3$ for the width and $l = 4$ for the shift.

The contribution of the Feshbach resonances, which only concern ionized atoms, is only important at low energies.

4.3.2. Ion Collisions

The two examples cited here (Tables 4 and 6) illustrate the following. For radiating ions, due to the Coulomb repulsion, the contribution of strong collisions is generally small. It increases with the temperature, because the Coulomb repulsion decreases. The contribution of inelastic collisions is very small for the same reason. Of course, there are no Feshbach resonances. The contribution of the quadrupole potential is predominant.

For neutrals, the situation is different, since there is no Coulomb repulsion. However, the contribution of inelastic collisions remains generally weak, and the contribution of the quadrupolar interaction is important, except when high levels are involved [31].

4.4. Accuracy of the SCP Method

The accuracy of a theoretical method is difficult to assess. Therefore, we estimate the accuracy of the SCP method by comparing to the experimental results. This has been made in all our papers that are cited in the STARK-B database. As examples, we will only cite here [9,35–39]. In spite of the fact that the strong collision contribution is never very small (see Tables 3–5), the accuracy is about 20%–30% for the widths of simpler spectra, but is worse for very complex spectra, particularly when configuration mixing is present in the description of energy levels, but not always [39]. If the shifts are of the same order of magnitude as the widths, their accuracy are similar to that of the widths. If they are smaller or much smaller, their accuracy is worse, because of the cancellation effects between the initial and final level. However, such an accuracy is enough for the needs of stellar physics and laboratory physics.

We note that within the semiclassical perturbation method, the weak inelastic collisions are the most reliable. Therefore, especially when their contribution is dominant, the obtained results are of good accuracy. Since the more sophisticated close-coupling method is not suitable for large-scale calculations, semiclassical perturbation data are still the best available data in many cases.

4.5. Ab Initio and Automatic Codes for Obtaining a Great Number of Data in a Same Run and the Influence of the Chosen Atomic Structure

For obtaining widths and shifts of a given line, in addition to the charges Z_A, Z_P, the chosen temperatures and densities, one must also input the energy levels and the $\langle r \rangle$ of the initial, final levels of the line and all the perturbing levels, and the oscillator strengths between the initial and all the perturbing levels. The $\langle r \rangle^2$ and B_i, B_f, B_{if} values of the initial and final levels also have to be input. The results of Stark broadening parameters determination performed by Dimitrijević, Sahal-Bréchot *et al.* using the semiclassical perturbation method are contained in more than 130 publications and have been

implemented in the STARK-B database [15]. Thanks to the creation of *ab initio* [40], automatic codes coupling the atomic data and the SCP code, more than several hundred lines (and sometimes about one thousand) can be treated in a same run. The calculations are very fast: only one night is sufficient with a laptop for treating several hundred lines in a same run for several temperatures and densities.

In the older papers, the energies of the levels were taken from measurements and various publications, and the oscillator strengths were obtained using the Coulomb approximation with the quantum defect (Bates and Damgaard approximation, [41], improved for high n values by [42]). As the $\langle r \rangle$, the $\langle r \rangle^2$ were obtained by means of the hydrogenic value with a quantum defect.

Then TOPbase has often been used since the 1990s [43], when the needed sets of energy levels and oscillator strengths became available: see, e.g., [35] and further papers, e.g., [38]. The TOPbase atomic data have been obtained within the close-coupling scattering theory by means of the R-matrix method with innovative asymptotic techniques. Thus they are especially appropriate for low and moderately ionized light atoms, because LS coupling is assumed.

Since the turn of the century, the SUPERSTRUCTURE (SST) code [44] has been used for ionized atoms, e.g., [45] and further papers. SST is well suited for moderately and highly charged ions. The wave functions are determined by the diagonalization of the nonrelativistic Hamiltonian using orbitals calculated in a scaled Thomas–Fermi–Dirac–Amaldi potential. Relativistic corrections are introduced according to the Breit–Pauli approach. Atomic data are obtained in intermediate coupling.

The Cowan code [46] is interesting for complex atoms and has been coupled to the SCP code [39]. The Cowan code, based on a Hartree–Fock–Slater multi-configuration expansion method with statistical exchange, contains relativistic corrections treated by perturbations. Therefore, this method is especially suited to neutral and moderately-ionized heavy atoms. The Cowan code is also useful, because the $\langle r \rangle$ and the $\langle r \rangle^2$ are provided, and then, we can use better values than the hydrogenic ones.

The difference between the use of the different atomic data codes does not exceed 30%, except in exceptional cases, such as in [38], for instance (see below).

Si V and Ne V line widths and shifts data have been calculated with both Bates and Damgaard and SST atomic data [45,47]. The difference does not exceed 30%. C II widths and shifts data have been calculated with both TOPbase and Bates and Damgaard atomic data, [38], and the difference does not exceed a few percent, except when configuration interaction plays an important role by allowing a forbidden transition.

Notice that widths and shifts due to positive ion impacts can be, in certain cases, larger than those due to electron impacts: for Cr I lines studied in [30], there are perturbing levels that are very close to the upper initial ones (4.26 and 14.14 cm^{-1}). This special situation is due to configuration interaction effects.

This gives an idea of the importance of the chosen atomic structure for obtaining Stark broadening data.

4.6. Modifications in Progress and Prospects

Until now, the B_i, B_f, B_{if} coefficients have been "manually" calculated before entering the input data of the code. A new subroutine is in progress, which will automatically calculate these coefficients in the code.

It would be also interesting to study the difference obtained in the SCP results by introducing the large and small ξ asymptotic expansions provided in [48].

To continue on the same train of thought, it would be interesting to include penetrating orbits in the SCP method and code. The difference between the SCP method and the close-coupling ones is considered to be due to close collisions, which should be overestimated by the SCP method. Penetrating orbits were included in semiclassical calculations [49,50], and the discrepancies between quantal and semiclassical calculations became much smaller. However, our SCP method provides results that are in agreement within 20%–30% with the experimental results, whereas the majority of the most accurate (close-coupling) quantum results disagree within a factor of roughly two ([36,37] and references to close-coupling calculations therein). This remains unexplained.

4.7. Regularities and Systematic Trends

Regularities and systematic trends have been observed for many years. A number of them can be understood and, thus, predicted by looking at the formulae provided by the SCP method. This can be easily checked by using the SCP data provided by STARK-B [15], for instance. Some of them are discussed in [31].

In order to interpret the regularities, the widths and shifts data must be expressed in frequency (or angular frequency) units and not in units of wavelength. We will discuss the principal systematic trends in the following.

4.7.1. Behavior with temperature

(1) High temperatures:

At high temperatures (or very small $\Delta E_{ii'}$), the Coulomb attraction or repulsion for ion emitters is small; the behavior is the same for neutrals and ions: $a(z)$ behaves as $ln(E)$, and thus, the cross-sections as $(\mu/m_e)ln(E)/E$. With a rough reasoning, it can be deduced that the widths decrease as $\sqrt{\mu/m_e}\,ln(T)/T$; *cf.* in particular [51,52]. In addition, due to the mass effect, the contribution of the ion colliders can be greater than that of electrons, e.g., [30].

(2) Low temperatures:

At low temperatures, the behavior is different for neutral and ion emitters. For ions colliding with electrons, the collision strengths tend towards a finite limit; the cross-sections decrease as $1/E$ near the threshold, and the width decreases as $1/\sqrt{T}$. For neutrals colliding with electrons, the width begins to increase with the temperature.

4.7.2. Behavior with the charge of the perturber

As expected by the SCP formulae, the shifts increase linearly with Z_P; *cf.* [53] for instance.

4.7.3. Behavior with the charge of the radiating ion

The widths are predicted to vary as Z_{eff}^{-2}, with $Z_{eff} = Z_A + 1$. This is shown in [37], for instance; *cf.* Figure 20 of that paper, which shows a -1.84 slope for the $3s - 3p$ transitions from C IV to P XIII. This is due to the behavior of the line strengths (and, thus, oscillator strengths) with the charge of the radiating ion in the Coulomb approximation.

4.7.4. Behavior of the width of a spectral series of transitions of a given neutral or ionized atom with increasing principal quantum number n

Due to the behavior of the dipolar line strengths in the Coulomb approximation, it is expected that the width of a spectral series $n_1\, l_1 \, - \, n\, l$ increases as n^4, when the principal quantum number, n, increases. This has been verified; *cf.* [38,39], for instance.

The dependence of the broadening parameters of spectral lines due to impacts with charged particles *versus* the principal quantum number within a spectral series is important information. If we know the trend of Stark broadening parameters within a spectral series, it is possible to interpolate or extrapolate the eventually missing values within the considered series.

4.7.5. Importance of the fine-structure splitting

Finally, it will be pointed out that the behaviors of the fine structure widths of a multiplet are not very sensitive to the fine structure splitting: for the $3s - 3p$ multiplets of the Li-like series, the ratio of the widths of the two components only attains 1.12 for P XIII [37]. This is quite negligible by looking at the accuracy of the calculations.

5. Conclusions

The SCP code is now extensively used for the needs of spectroscopic diagnostics and modeling, and the results of the published calculations are displayed in the STARK-B database, [15]. Data for 123 neutral and ionized atoms (49 chemical elements) are currently included in STARK-B. In the present paper, we have presented the main approximations leading to the impact semiclassical perturbation method, and we have given the formulae entering the numerical SCP code. This would permit us to better understand the validity conditions of the method and of the results; and also to understand and predict some regularities and systematic trends. If we know the systematic trends of the Stark broadening parameters, it would be possible to interpolate or extrapolate the existing and provided data for obtaining missing values.

This would also allow us to compare the method and its results to those of other methods and codes.

Acknowledgments

The support of IAEA is gratefully acknowledged. The support of the Ministry of Education, Science and Technological Development of Republic of Serbia through projects 176002 and III44022 is also acknowledged. This work has also been supported by the Paris Observatory, the CNRS and the PNPS (Programme National de Physique Stellaire, INSU-CNRS). The cooperation agreements between

Tunisia (DGRS) and France (CNRS) (project code 09/R 13.03, No.22637) are also acknowledged. This paper has also been written within the LABEX Plas@par project and received financial state aid managed by the Agence Nationale de la Recherche, as part of the programme "Investissements d'avenir" under the reference, ANR–11–IDEX–0004–02.

Author Contributions

The original method and the associated code was created and developed by S. Sahal-Bréchot during the sixties and seventies [5–9]. M.S. Dimitrijević has contributed to update and operate the code since the eighties [10–12,28] and further papers. In particular, he developed during this decade the automatic code coupled to the Bates and Damgaard's oscillator strengths leading to more than one hundred widths and shifts in a same run. Then N. Ben Nessib joined the cooperation in the second part of the nineties. In particular, he extended in the beginning of this new century the quadrupole part of the width to very complex atoms with one of his Tunisian's PhD's student [13]. Then he developed with the Tunisian team the coupling of the SCP code to TOPbase ([43]), to SST [44] and to the Cowan code [46]. This allowed to obtain "*ab initio*" codes [40] permitting to obtain several hundred widths and shifts data in a same run e.g., [38,39,45]. All the resulting data and publications appear in the database STARK-B [15].

Conflicts of Interest

The authors declare no conflict of interest

References

1. Baranger, M. Simplified Quantum-Mechanical Theory of Pressure Broadening. *Phys. Rev.* **1958**, *111*, 481–493.
2. Baranger, M. Problem of Overlapping Lines in the Theory of Pressure Broadening. *Phys. Rev.* **1958**, *111*, 494–504.
3. Baranger, M. General Impact Theory of Pressure Broadening. *Phys. Rev.* **1958**, *112*, 855–865.
4. Baranger, M. Spectral Line Nroadening in Plasmas. In *Atomic and Molecular Processes*; Bates, D.R., Ed.; Academic Press: New-York, NY, USA; London, UK, 1962; pp. 493–548.
5. Bréchot, S. On electron impact broadening of positive ion lines. *Phys. Lett. A*, **1967**, *24A* 476–477.
6. Sahal-Bréchot, S. Impact theory of the broadening and shift of spectral lines due to electrons and ions in a plasma. *Astron. Astrophys.* **1969**, *1*, 91–123.
7. Sahal-Bréchot, S. Impact theory of the broadening and shift of spectral lines due to electrons and ions in a plasma (continued). *Astron. Astrophys.* **1969**, *2*, 322–354.
8. Sahal-Bréchot, S. Stark nroadening of isolated lines in the impact approximation. *Astron. Astrophys.* **1974**, *35*, 319–321.
9. Fleurier, C.; Sahal-Bréchot, S.; Chapelle, J. Stark profiles of some ion lines of alkaline earth elements. *J. Quant. Spectroscop. Ra.* **1977**, *17*, 595–603.
10. Dimitrijević, M.S.; Sahal-Bréchot, S. Stark broadening of neutral helium lines. *J. Quant. Spectroscop. Ra.* **1984**, *31*, 301–313.

11. Dimitrijević, M.S.; Sahal-Bréchot, S.; Bommier, V. Stark broadening of spectral lines of multicharged ions of astrophysical interest. I - C IV lines. *Astron. Astrophys.* **1991**, *89*, 581–590.
12. Dimitrijević, M.S.; Sahal-Bréchot, S.; Bommier, V. Stark broadening of spectral lines of multicharged ions of astrophysical interest. II- Si IV lines. *Astron. Astrophys.* **1991**, *89*, 591–598.
13. Mahmoudi, W.F.; Ben Nessib, N.; Sahal-Bréchot, S. Stark broadening of isolated lines: Calculation of the diagonal multiplet factor for complex configurations ($n_1l_1^n$ $n_2l_2^m$ $n_3l_3^p$). *Eur. Phys. J. D* **2008**, *47*, 7–10.
14. Seaton, M.J. The Impact parameter method for electron excitation of optically allowed atomic transitions. *Proc. Phys. Soc.* **1962**, *79* , 1105–1117.
15. Sahal-Bréchot, S.; Dimitrijević, M.S.; Moreau, N. STARK-B Database. LERMA, Observatory of Paris, France and Astronomical Observatory: Belgrade, Serbia, 2014. Available online: http://stark-b.obspm.fr (accessed on 21 April 2014).
16. Mihalas, D. *Stellar Atmospheres*; W. H. Freeman and Company: San Francisco, CA, USA, 1978; pp. 29 and 411–446.
17. Omont, A.; Smith, E.W.; Cooper, J. Redistribution of resonance radiation. I. The effect of collisions. *Astrophys. J.* **1972**, *175*, 185–199.
18. Bommier, V. Master equation theory applied to the redistribution of polarized radiation, in the weak radiation field limit. I. Zero magnetic field case. *Astron. Astrophys.* **1997**, *328*, 706–725.
19. Alder, A.; Bohr, A.; Huus, B.; Mottelson, B.; Winther, A. Study of nuclear structure by electromagnetic excitation with accelerated ions. *Rev. Mod. Phys.* **1956**, *28*, 433–542.
20. Seaton, M.J. Excitation of coronal lines by proton impact. *Mon. Not. R. Astron. Soc.* **1964**, *127*, 191–194.
21. Klarsfeld, S. Exact calculation of electron-broadening shift functions. *Phys. Lett. A* **1970**, *32A*, 26–27.
22. Bréchot, S.; van Regemorter, H. L'élargissement des raie spectrales par chocs. 1.- La contribution adiabatique. *Ann. Astroph.* **1964**, *27*, 432–449.
23. Press, W.H.; Teukolsky, S.A.; Vetterling, W.T.; Flannery, B.F. *Numerical Recipes in Fortran, The Art of Scientific Computing*, 2nd ed.; Cambridge University Press: New York, NY, USA, 1992; pp. 229–233.
24. Feautrier, N. Calcul semi-classique des sections d'excitation par chocs électroniques pour les ions. Application à l'élargissement des raies. *Ann. Astroph.* **1968**, *31*, 305–309.
25. Griem, H.R. *Spectral Line Broadening by Plasmas*; Academic Press: New York, NY, USA; London, UK, 1974.
26. Watson, G.N. *A Treatise on the Theory of Bessel Functions*; Cambridge University Press: London, UK, 1966.
27. Bateman, H. Higher transcendental functions. In *Bateman Manuscript Project*; Erdelyi, A., Ed.; McGraw-Hill: New York, NY, USA, 1953–1955; Volume 2, p. 88.
28. Dimitrijević, M.S.; Sahal-Bréchot, S. Asymptotic behavior of the A and a functions for ionized emitters in semiclassical Stark-broadening theory. *J. Quant. Spectroscop. Ra.* **1992**, *48*, 349–351.
29. Klarsfeld, S. On Stark broadening functions for nonhydrogenic ions. *Phys. Lett. A* **1970**, *33A*, 437–438.

30. Dimitrijević, M.S.; Ryabchikova, T.; Popović, L.Č.; Shulyak, D.; Khan, S. On the influence of Stark broadening on Cr I lines in stellar atmospheres. *Astron. Astrophys.* **2005**, *435*, 1191–1198.
31. Sahal-Bréchot, S.; Dimitrijević, M.S.; Ben Nessib, N. Comparisons and Comments on Electron and Ion Impact Profiles of Spectral Lines. *Balt. Astron.* **2011**, *20*, 523–530.
32. Stehlé, C.; Mazure, A.; Nollez, G.; Feautrier, N. Stark broadening of hydrogen lines: New results for the Balmer lines and astrophysical consequences. *Astron. Astrophys.* **1983**, *127*, 263–266.
33. Elabidi, E.; Sahal-Bréchot, S.; Ben Nessib, N. Fine structure collision strengths for S VII lines. *Phys. Scripta* **2012**, *85*, 065302:1–065302:13.
34. Dimitrijević, M.S.; Feautrier, N.; Sahal-Bréchot, S. Comparison between quantum and semiclassical calculations of the electron impact broadening of the Li I resonance line. *J. Phys. B* **1981**, *14*, 2559–2568.
35. Dimitrijević, M.S.; Sahal-Bréchot, S. Stark broadening of Mg I spectral lines. *Phys. Scripta* **1995**, *52*, 41–51.
36. Elabidi, E.; Ben Nessib, N.; Cornille, M.; Dubau, J.; Sahal-Bréchot, S. Electron impact broadening of spectral lines in Be-like ions: Quantum calculations. *J. Phys. B* **2008**, *41*, 025702:1–025702:11.
37. Elabidi, H.; Sahal-Bréchot, S.; Ben Nessib, N. Quantum Stark broadening of 3s-3p spectral lines in Li-like ions; Z-scaling and comparison with semi-classical perturbation theory. *Eur. Phys. J. D* **2009**, *54*, 51–64.
38. Larbi-Terzi, N.; Sahal-Bréchot S.; Ben Nessib, N.; Dimitrijević, M.S. Stark-broadening calculations of singly ionized carbon spectral lines. *Mon. Not. R. Astron. Soc.* **2012**, *423*, 766–773.
39. Hamdi, R.; Ben Nessib, N.; Dimitrijević, M.S.; Sahal-Bréchot S. Stark broadening of Pb IV spectral lines. *Mon. Not. R. Astron. Soc.* **2013**, *431*, 1039–1047.
40. Ben Nessib, N. Ab initio calculations of Stark broadening parameters. *New Astron. Rev.* **2009**, *53*, 255–258.
41. Bates, D.R.; Damgaard, A. The calculation of the absolute strengths of spectral lines. *Trans. Roy. Soc. Lond.* **1949**, *242*, 101–122.
42. Van Regemorter, H.; Hoang Binh, Dy.; Prudhomme, M. Radial transition integrals involving low or high effective quantum numbers in the Coulomb approximation. *J. Phys. B* **1979**, *12*, 1053–1061.
43. Cunto, W.; Mendoza, C.; Ochsenbein, F.; Zeippen, C.J. TOPbase at the CDS. *Astron. Astrophys.* **1993**, *275*, L5–L8.
44. Eissner, W.; Jones, M.; Nussbaumer, H. Techniques for the calculation of atomic structures and radiative data including relativistic corrections. *Comp. Phys. Com.* **1974**, *8*, 270–306.
45. Ben Nessib, N.; Dimitrijević, M.S.; Sahal-Bréchot, S. Stark broadening of the four times ionized silicon spectral lines. *Astron. Astrophys.* **2004**, *423*, 397–400.
46. Cowan R.D.; Robert, D. Cowan's Atomic Structure Code. *The Theory of Atomic Structure and Spectra*; University of California Press: Berkeley, CA, USA, 1981. Available online: https://www.tcd.ie/Physics/people/Cormac.McGuinness/Cowan/ (accessed on 21 April 2014).
47. Hamdi, R.; Ben Nessib, N.; Dimitrijević, M.S.; Sahal-Bréchot, S. Stark broadening of the spectral lines of Ne V. *Astrophys. J. Suppl. S.* **2007**, *170*, 243–250.

48. Alexiou, S. Calculations of the semiclassical Stark broadening dipole width functions for isolated ion lines. *J. Quant. Spectroscop. Ra.* **1994**, *51*, 849–852.
49. Alexiou, S.; Glenzer, S.; Lee, R.W. Line shape measurement and isolated line width calculations: Quantal versus semiclassical methods. *Phys. Rev. E* **1999**, *60*, 6238–6240.
50. Alexiou, S.; Lee, R.W. Semiclassical calculations of line broadening in plasmas: Comparison with quantal results. *J. Quant. Spectroscop. Ra.* **2006**, *99*, 10–20.
51. Zmerli, B.; Ben Nessib, N.; Dimitrijević, M.S. Temperature dependence of atomic spectral line widths in a plasma. *Eur. Phys. J. D* **2008**, *48*, 389–395.
52. Elabidi, E.; Sahal-Bréchot, S. Checking the dependence on the upper level ionization potential of electron impact widths using quantum calculations. *Eur. Phys. J. D* **2011**, *61*, 285–290.
53. Dimitrijević, M.S. Stark broadening data tables for some analogous spectral lines along Li and Be isoelectronic sequences. *Serb. Astron. J.* **1999**, *159*, 65–72.